

Supplementary Information

Optimizing PtFe Intermetallics for Oxygen Reduction Reaction: From DFT Screening to In-Situ XAFS Characterization

Mingxing Gong,^a Jing Zhu,^a Mingjie Liu,^c Peifang Liu,^b Zhiping Deng,^a Tao Shen,^a Tonghui Zhao,^a Ruoqian Lin,^c Yun Lu,^a Shize Yang,^c Zhixiu Liang,^d Seong Min Bak,^d Eli Stavitski,^e Qin Wu,^c Radoslav R. Adzic,^d Huolin L. Xin,^{*, c, f} and Deli Wang^{*, a}

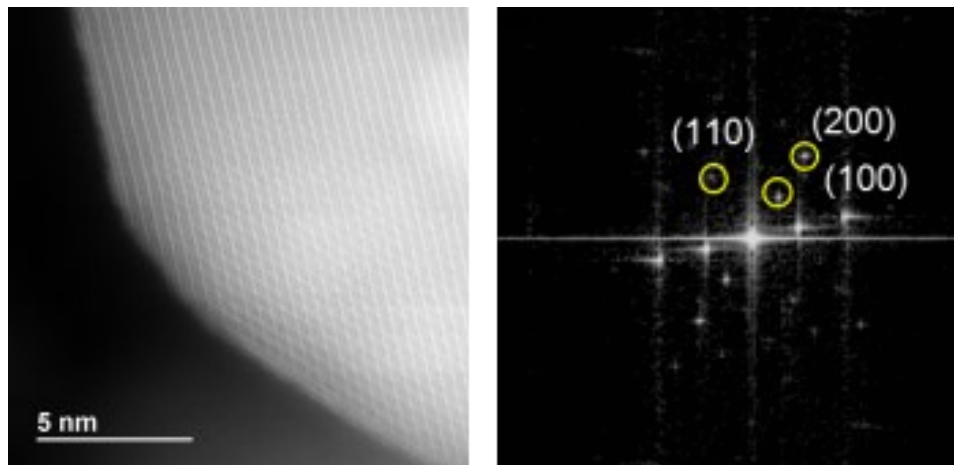


Figure S1. HRTEM image and corresponding diffractogram of O-Pt₃Fe.

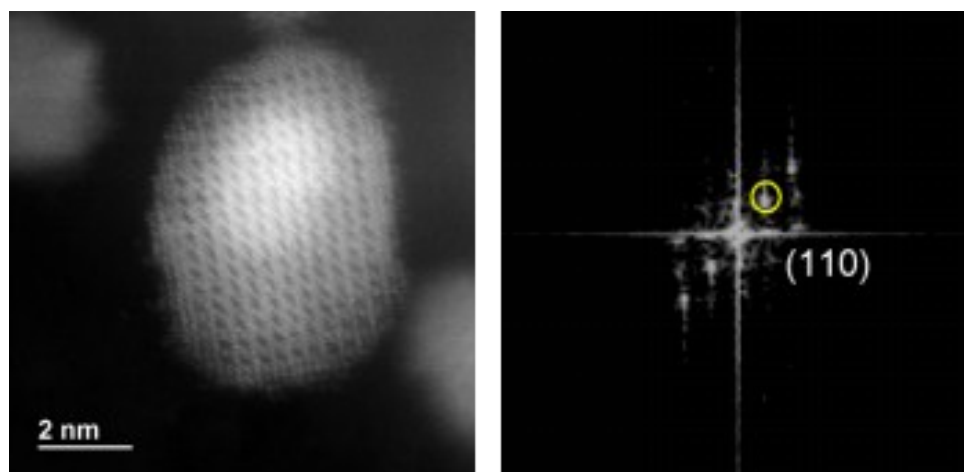


Figure S2. HRTEM image and corresponding diffractogram of O-PtFe.

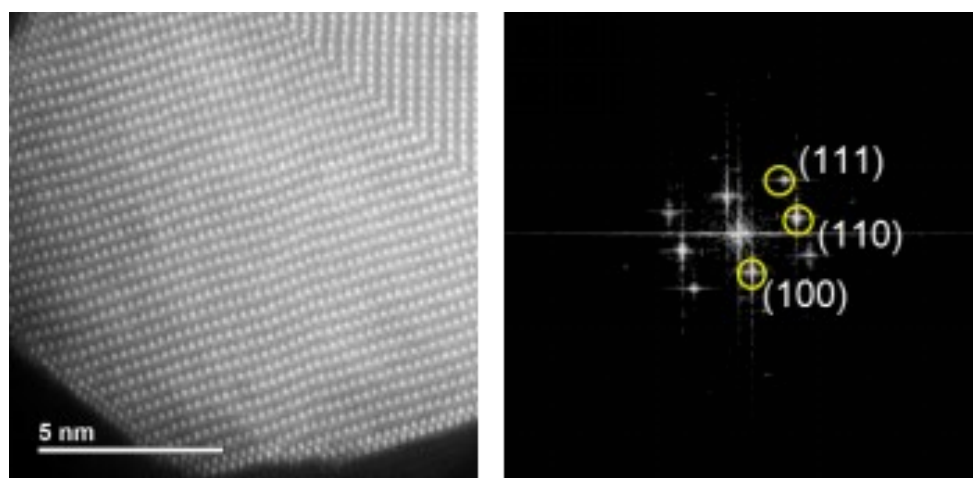


Figure S3. HRTEM image and corresponding diffractogram of O-PtFe₃.

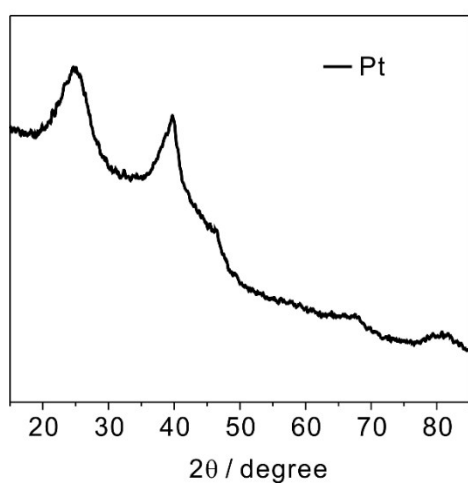


Figure S4. XRD pattern of Pt/C.

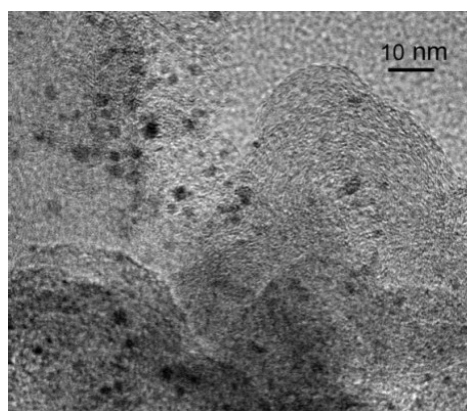


Figure S5. TEM image of Pt/C.

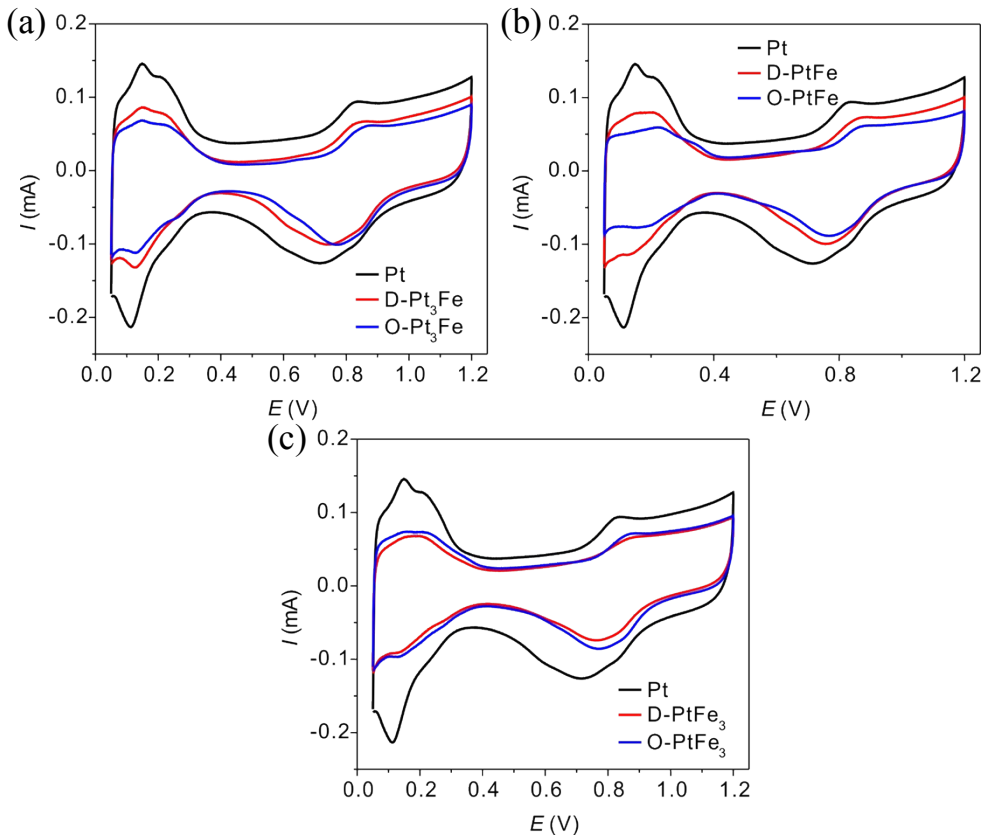


Figure S6. CVs of disordered and ordered Pt₃Fe (a), PtFe (b) and PtFe₃ (c) catalysts in 0.1 M HClO₄ purged with N₂ at a sweep rate of 50 mV s⁻¹.

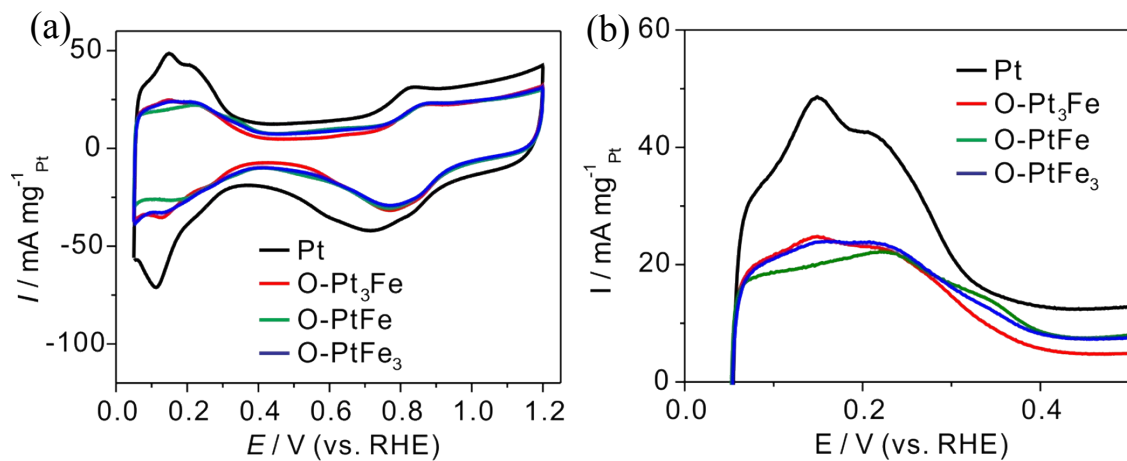


Figure S7. The CVs (a) and the enlarged region of hydrogen adsorption/desorption peaks (b) of ordered Pt-Fe and Pt catalysts.

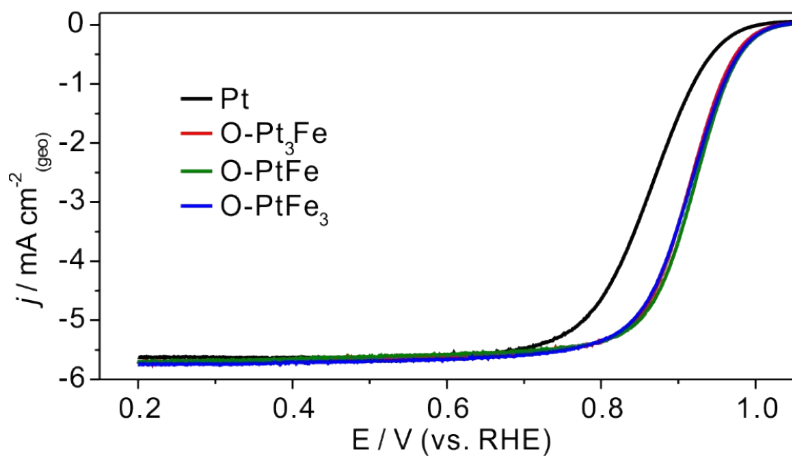


Figure S8. ORR polarization curves of ordered Pt-Fe in O₂-saturated 0.1 M HClO₄ solution.

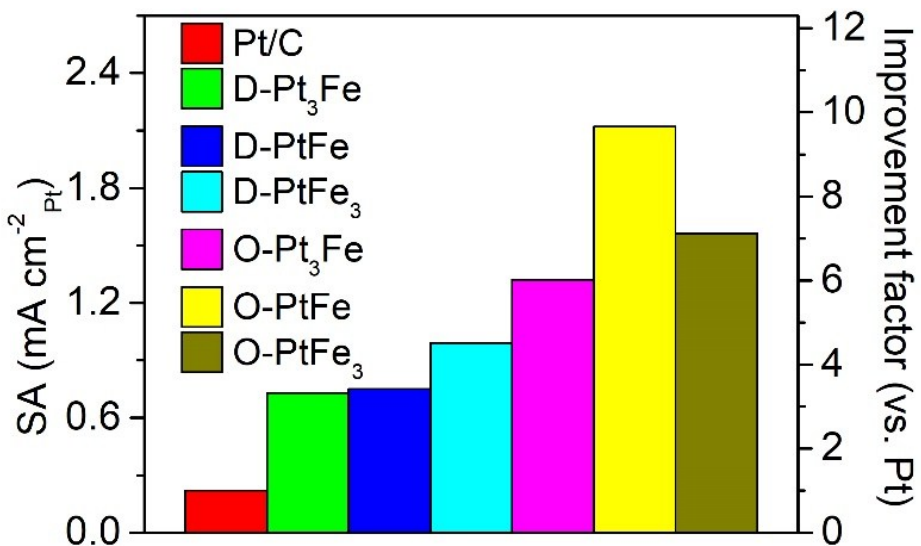


Figure S9. The SA comparison of all Pt-Fe and Pt catalysts.

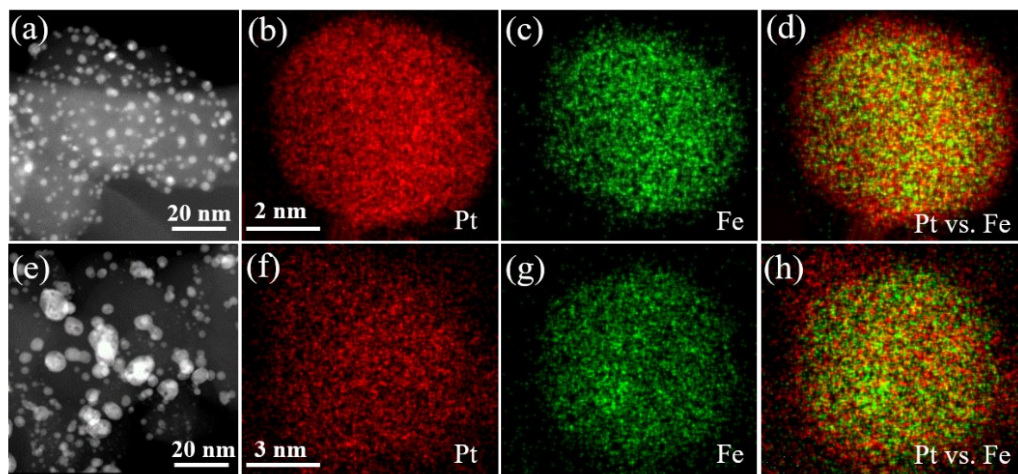


Figure S10. STEM image (a) and elemental mapping images (b-d) of O-PtFe NP after ADT. STEM image (e) and elemental mapping images (f-h) of D-PtFe NP after ADT.

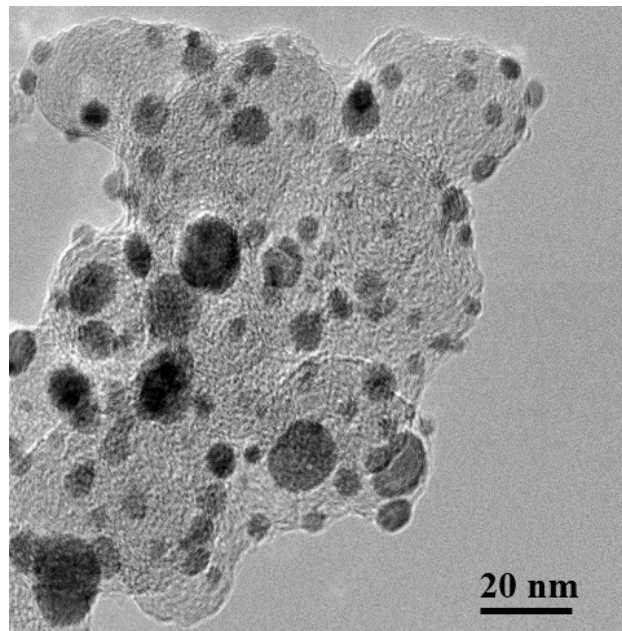


Figure S11. TEM image of Pt/C after ADT

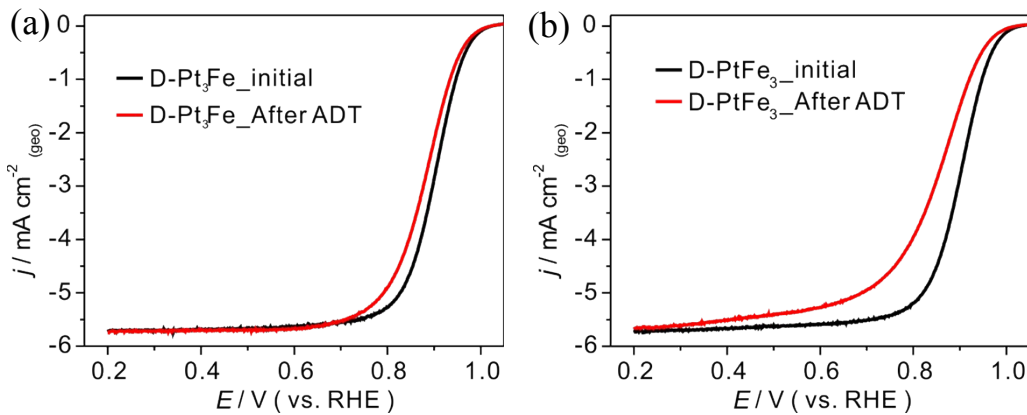


Figure S12. ORR polarization curves of D-Pt₃Fe (a) and D-PtFe₃ (b) before and after ADT.

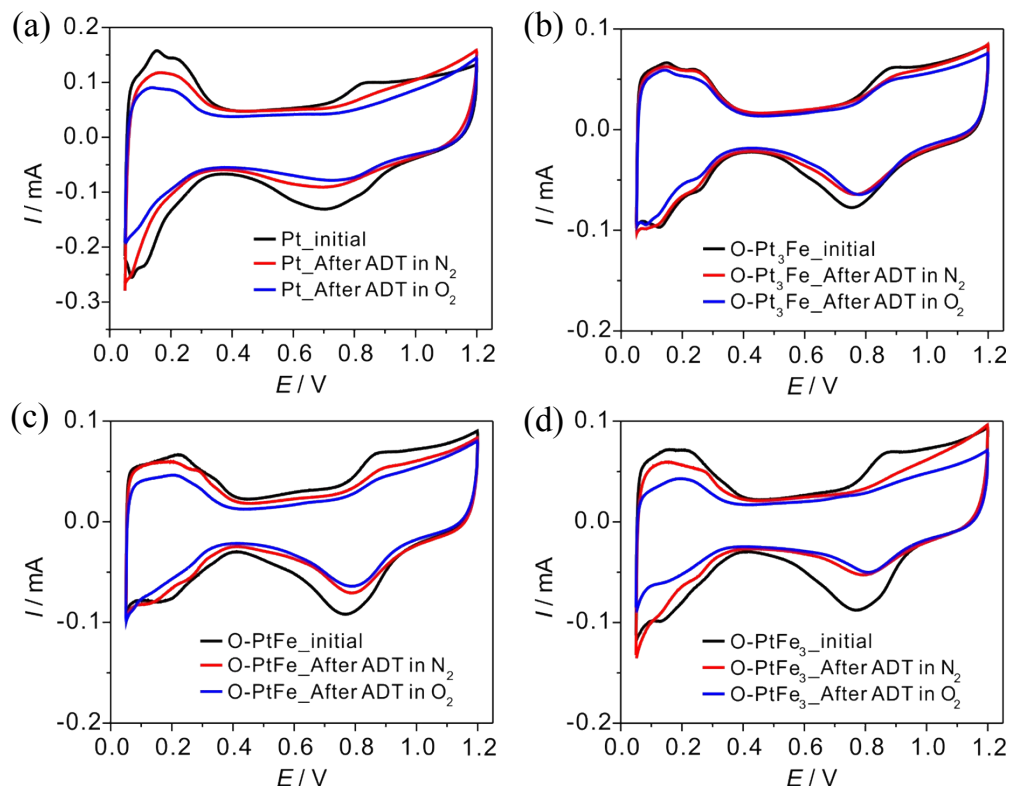


Figure S13. CVs of Pt (a), O-Pt₃Fe (b), O-PtFe (c), O-PtFe₃ (d) before and after ADT in N₂-purged and O₂-purged 0.1 M HClO₄ solution.

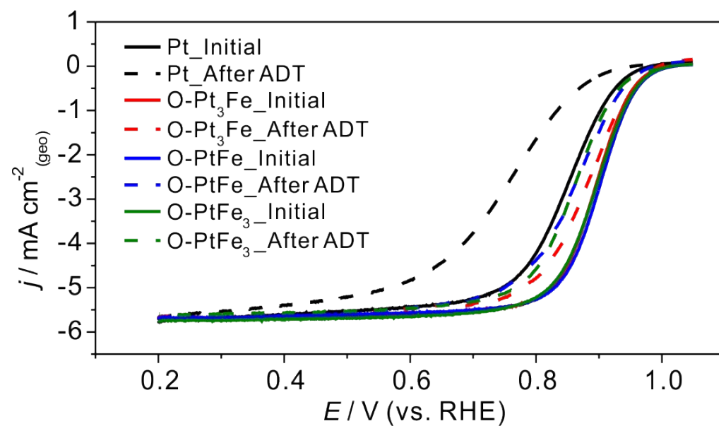


Figure S14. ORR polarization curves of ordered Pt-Fe catalysts and Pt before and after ADT in O₂-purged 0.1 M HClO₄ solution.

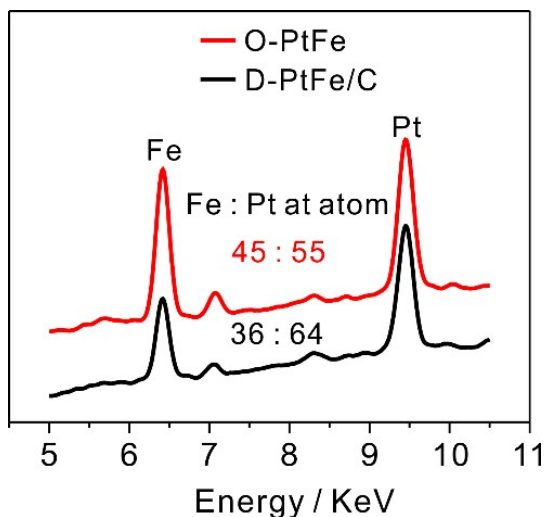


Figure S15. XRF patterns of D-PtFe and ordered O-PtFe after ADT.

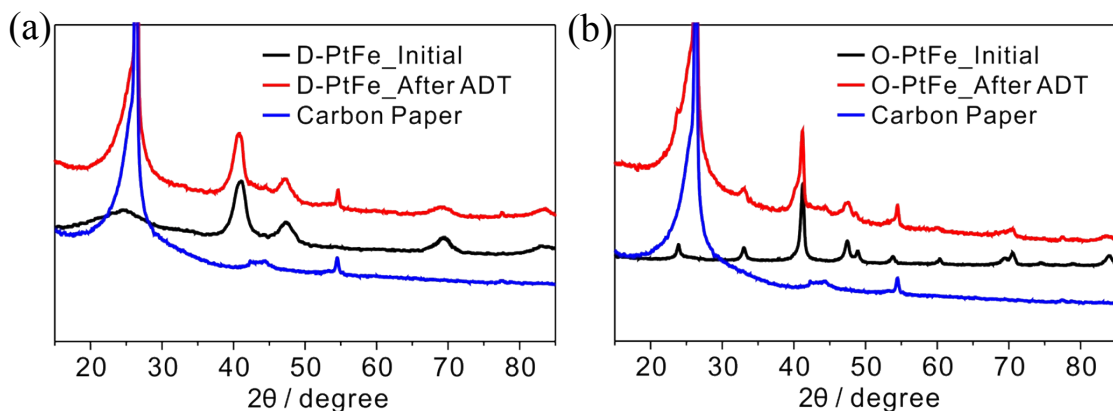


Figure S16. XRD patterns of D-PtFe (a) and O-PtFe (c) before and after ADT.

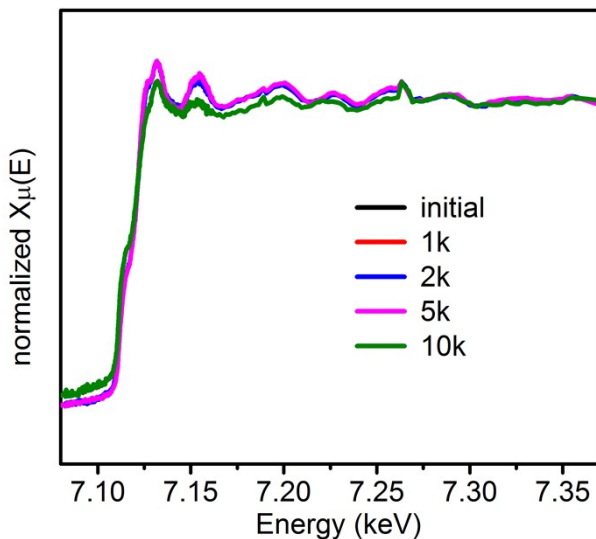


Figure S17. Fe K-edge XANES spectra of O-PtFe under ADT cycles.

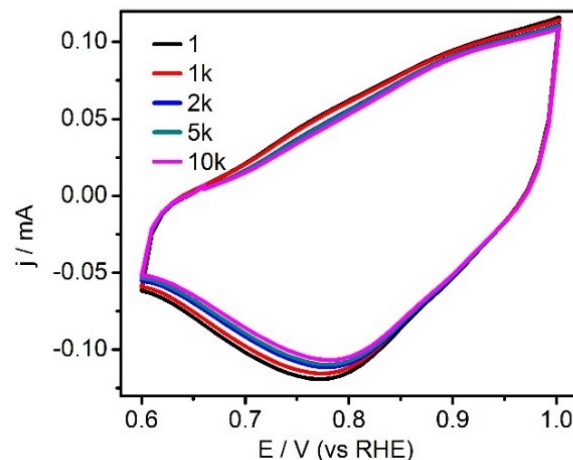


Figure S18. ADT cycles between 0.6-1.0 V during the in-situ XAFS experiment.

Table S1. XRD results of disordered and ordered Pt-Fe/C.

	2θ (220), deg.	domain size, nm	lattice param., nm
Pt	67.532	3	0.3916
D-Pt ₃ Fe	68.475	4.6	0.3868
D-PtFe	69.297	4.4	0.3821
D-PtFe ₃	69.927	4	0.38
O-Pt ₃ Fe	68.877	6.3	0.3852
O-PtFe	69.322	9.1	0.3828 (a), 0.3718 (c)
O-PtFe ₃	71.606	5.3	0.3724

Table S2. Comparison of the specific and mass activity toward ORR at 0.9 V for various intermetallic compounds as catalysts in 0.1 M HClO₄ from literatures.

Number	Catalyst	Temperatuue (°C)	Activity @0.9V	Improvement factor (vs. Pt)	Ref.
1	PtFe	RT	0.37 mA cm ⁻² _{Pt}	5.3	1
			0.26 A mg ⁻¹ _{Pt}	7.4	
2	PtFe	60	0.7 A mg ⁻¹ _{Pt}	5.4	2
3	PtFe	25	1.6 A mg ⁻¹ _{Pt}	11.4	3
			2.3 mA cm ⁻² _{Pt}	10.5	
4	PtFe		3.16 mA cm ⁻² _{Pt}	11.3	4
5	Pt ₃ Fe ₂	RT	0.23 A mg ⁻¹ _{Pt}	2.3	5
			0.55 mA cm ⁻² _{Pt}	1.6	
6	Pt ₂ FeCu	RT	0.53 A mg ⁻¹ _{Pt}	2.5	6
			1.35 mA cm ⁻² _{Pt}	4	
7	Pt ₂ FeCo	RT	0.5 A mg ⁻¹ _{Pt}	2.2	7
	Pt ₆ FeCo	RT	0.27 A mg ⁻¹ _{Pt}	1.2	
8	Pt ₂ FeCo	RT	0.133 mA cm ⁻² _{Pt}	1.4	8
			0.067 A mg ⁻¹ _{Pt}	1.4	
9	Pt ₂ FeNi	RT	0.137 mA cm ⁻² _{Pt}	1.4	8
			0.068 A mg ⁻¹ _{Pt}	1.5	
10	Pt ₃ Co	RT	0.52 A mg ⁻¹ _{Pt}	8.7	9
			1.1 mA cm ⁻² _{Pt}	12	
11	AuPt ₄ Co ₅	RT	0.53 mA cm ⁻² _{Pt}	2	10
			0.68 A mg ⁻¹ _{Pt}	3.1	
12	Pt ₃ Cr	RT	0.45 mA cm ⁻² _{Pt}	2.3	11
13	Pt ₃ Al	25	1.23 mA cm ⁻² _{Pt}	6.3	12
14	PtFe	25	2.23 mA cm ⁻² _{Pt}	9.6	This work
			0.68 A mg ⁻¹ _{Pt}	4.8	

Table S3. EXAFS fitting results of the D-PtFe and O-PtFe

Results Samples \	Bond	CN	R(Å)	$\sigma^2(\text{\AA}^2) \cdot 10^{-3}$	$\Delta E_0(\text{eV})$
D-PtFe	Pt-Pt	8(6)	2.739(4)	3.6(2)	3.1(1)
	Pt-Fe	5(8)	2.652(3)		
	Fe-Pt	6(2)	2.652(1)	4.0(8)	3.4(2)
	Fe-Fe	2(6)	2.701(7)		
O-PtFe	Pt-Pt	7(6)	2.708(6)	2.7(3)	3.6(5)
	Pt-Fe	6(4)	2.621(5)		
	Fe-Pt	7(1)	2.621(4)	3.1(6)	1.8(9)
	Fe-Fe	2(3)	2.693(5)		

CN stands for coordination number; R is the bond length; σ^2 parameter is the Debye-Waller factor and reflects the structural disorder of the test sample, including dynamic disorder from thermal motion of the atoms and static disorder from packing defects. The ΔE_0 parameter is the absorption edge energy shift; it represents the difference between the experimental E_0 energy and that calculated for the structural model used to fit the spectra.

Table S4. In-situ EXAFS fitting results of the O-PtFe during ADT.

Systems Cycles \ Bond	CN	R(Å)	$\sigma^2(\text{Å}^2) \cdot 10^{-3}$	$\Delta E_0(\text{eV})$
initial	Pt-Fe	6(6)	2.628(6)	2.8 (3)
	Pt-Pt	8(0)	2.722(1)	3.9 (2)
1k cycles	Pt-Fe	7(4)	2.621(4)	3.0 (7)
	Pt-Pt	6(8)	2.719(7)	3.8 (1)
2k cycles	Pt-Fe	7(4)	2.625(6)	3.2 (7)
	Pt-Pt	6(4)	2.721(5)	3.7(6)
5k cycles	Pt-Fe	6(6)	2.632(8)	3.4 (1)
	Pt-Pt	7(8)	2.723(2)	3.4 (3)
10k cycles	Pt-Fe	6(3)	2.628(1)	3.4 (3)
	Pt-Pt	7(6)	2.727(6)	3.3 (5)

REFERENCES

1. Du, X. X.; He, Y.; Wang, X. X.; Wang, J. N., Fine-grained and fully ordered intermetallic PtFe catalysts with largely enhanced catalytic activity and durability. *Energy & Environmental Science* 2016, 9, 2623-2632.
2. Li, J.; Xi, Z.; Pan, Y. T.; Spendelow, J. S.; Duchesne, P. N.; Su, D.; Li, Q.; Yu, C.; Yin, Z.; Shen, B.; Kim, Y. S.; Zhang, P.; Sun, S., Fe Stabilization by Intermetallic L10-FePt and Pt Catalysis Enhancement in L10-FePt/Pt Nanoparticles for Efficient Oxygen Reduction Reaction in Fuel Cells. *Journal of the American Chemical Society* 2018, 140, 2926-2932.
3. Chung, D. Y.; Jun, S. W.; Yoon, G.; Kwon, S. G.; Shin, D. Y.; Seo, P.; Yoo, J. M.; Shin, H.; Chung, Y. H.; Kim, H.; Mun, B. S.; Lee, K. S.; Lee, N. S.; Yoo, S. J.; Lim, D. H.; Kang, K.; Sung, Y. E.; Hyeon, T., Highly Durable and Active PtFe Nanocatalyst for Electrochemical Oxygen Reduction Reaction. *Journal of the American Chemical Society* 2015, 137, 15478-85.
4. Li, Q.; Wu, L.; Wu, G.; Su, D.; Lv, H.; Zhang, S.; Zhu, W.; Casimir, A.; Zhu, H.; Mendoza-Garcia, A.; Sun, S., New approach to fully ordered fct-FePt nanoparticles for

- much enhanced electrocatalysis in acid. *Nano letters* 2015, 15, 2468-73.
- 5. Prabhudev, S.; Bugnet, M.; Bock, C.; Botton, G. A., Strained lattice with persistent atomic order in Pt₃Fe₂ intermetallic core–shell nanocatalysts. *ACS nano* 2013, 7, 6103-6110.
 - 6. Arumugam, B.; Tamaki, T.; Yamaguchi, T., Beneficial Role of Copper in the Enhancement of Durability of Ordered Intermetallic PtFeCu Catalyst for Electrocatalytic Oxygen Reduction. *ACS applied materials & interfaces* 2015, 7, 16311-21.
 - 7. Tamaki, T.; Minagawa, A.; Arumugam, B.; Kakade, B. A.; Yamaguchi, T., Highly active and durable chemically ordered Pt–Fe–Co intermetallics as cathode catalysts of membrane–electrode assemblies in polymer electrolyte fuel cells. *Journal of Power Sources* 2014, 271, 346-353.
 - 8. Nguyen, M. T.; Wakabayashi, R. H.; Yang, M.; Abruña, H. D.; DiSalvo, F. J., Synthesis of carbon supported ordered tetragonal pseudo-ternary Pt 2 M'M'' (M = Fe, Co, Ni) nanoparticles and their activity for oxygen reduction reaction. *Journal of Power Sources* 2015, 280, 459-466.
 - 9. Wang, D.; Xin, H. L.; Hovden, R.; Wang, H.; Yu, Y.; Muller, D. A.; DiSalvo, F. J.; Abruna, H. D., Structurally ordered intermetallic platinum-cobalt core-shell nanoparticles with enhanced activity and stability as oxygen reduction electrocatalysts. *Nature materials* 2013, 12, 81-7.
 - 10. Kuttiyiel, K. A.; Kattel, S.; Cheng, S.; Lee, J. H.; Wu, L.; Zhu, Y.; Park, G.-G.; Liu, P.; Sasaki, K.; Chen, J. G., Au-doped Stable L10 Structured Platinum Cobalt Ordered Intermetallic Nanoparticle Catalysts for Enhanced Electrocatalysis. *ACS Applied Energy Materials* 2018, 1, 3771-3777.
 - 11. Cui, Z.; Chen, H.; Zhou, W.; Zhao, M.; DiSalvo, F. J., Structurally Ordered Pt₃Cr as Oxygen Reduction Electrocatalyst: Ordering Control and Origin of Enhanced Stability. *Chemistry of Materials* 2015, 27, 7538-7545.
 - 12. Lang, X.-Y.; Han, G.-F.; Xiao, B.-B.; Gu, L.; Yang, Z.-Z.; Wen, Z.; Zhu, Y.-F.; Zhao, M.; Li, J.-C.; Jiang, Q., Mesostructured Intermetallic Compounds of Platinum and Non-Transition Metals for Enhanced Electrocatalysis of Oxygen Reduction Reaction. *Advanced Functional Materials* 2015, 25, 230-237.